Transition-State Energy and Geometry, Exothermicity, and van der Waals Wells on the $F + H_2 \rightarrow FH + H$ Ground-State Surface Calculated at the r_{12}-ACPF-2 Level†

Wim Cardoen,‡ Robert Gdanitz,§ and Jack Simons*

Department of Chemistry and Henry Eyring Center for Theoretical Chemistry, University of Utah, Salt Lake City, Utah 84112

Received: May 4, 2005; In Final Form: August 12, 2005

Explicitly correlated averaged coupled-pair functional methods have been used to compute the ground-state Born−Oppenheimer potential energy surface for the $F + HH' \rightarrow FH + H'$ reaction at the $F + HH'$ and $FH + H'$ asymptotes, the F···HH′, and FH···H van der Waals wells, the reaction transition state, and at points along the intrinsic reaction coordinate connecting all of these stationary points. To these energies, corrections for spin−orbit coupling and scalar relativistic effects were added to produce total electronic energies whose accuracy is demonstrated to be very high (e.g., 0.1 kcal mol^{-1}). The final data are used to refine the two-body parts of the currently best three-dimensional potential energy surface for this reaction, to predict several spectroscopic parameters of the species involved, and to offer accurate estimates of the title reaction's exothermicity (32.0 kcal mol^{-1}) and activation barrier (1.8 kcal mol^{-1}) as well as the geometry of the transition state.

I. Introduction

In an earlier paper,[1] we detailed the current status of the comparison between experimentally observed reaction cross-sections and product HF(v,J) vibration−rotation state populations and corresponding results obtained using quantum scattering theory on current state-of-the-art potential energy surfaces (PESs) for the title reaction. More recently, a paper from the Skodje group has appeared[2] that offers an even more up-to-date evaluation and an excellent overview. The latter paper points out that remaining experimental−theoretical differences are unlikely to arise from the treatment of the quantum dynamics or through contributions of the $^2P_{1/2}$ excited state of fluorine, which is in line with what we said in ref 1. Reference 2 also emphasizes that differences in the HF product vibrational populations likely arise from an incorrect exothermicity of the theoretical PES and that there seem to be errors in this PES in the region of the product-channel FH···H van der Waals well. The main emphasis of ref 2 was to introduce corrections to the Stark and Werner[3] PES, which is the best global three-dimensional (3D) PES presently available, and to improve its descriptions of the exothermicity and of the FH···H van der Waals well.

Although great progress has been made on both the experimental and theoretical (PES and reaction dynamics) fronts in the past 20 years, there remain differences between the theoretical and experimental findings suggesting that small errors (ca. 0.5−1.0 kcal mol^{-1}) remain in even the very best current PES and that these small errors limit scientists' ability to obtain a quantitatively accurate agreement between experimental observations and cutting-edge theoretical simulations.

In ref 1, we showed how to systematically construct a proper (i.e., allowing for correct bond breaking and forming as well as for essential electron correlations) active space (AS) of reference electronic configurations for use in computing the energy of FH_2 at geometries characteristic of critical points on and the intrinsic reaction path of the title reaction's PES. In subsequent configuration interaction (CI) and averaged coupled-pair functional (ACPF-2) calculations,[1] we used an AS of configurations to compute the ground-state Born−Oppenheimer electronic energy at the $F + H_2$ reactant, F···H_2 and FH···H van der Waals minima, transition-state, and FH + H product geometries. We demonstrated that this choice of configurations and CI/ACPF-2 methodologies can both avoid symmetry breaking artifacts and yield accuracies for $F + H_2 \rightarrow FH + H$ comparable to the PES of Stark and Werner (SW), which is presently the best available and which is the PES for which ref 2 offers product-channel corrections. However, even using such correlated electronic structure methods with large atomic orbital basis sets and carefully chosen ASs, there remain small differences (0.5−1.0 kcal mol^{-1}) among our resulting data,[1] the SW energies, and related experimental data (e.g., in the reaction exothermicity). There also are substantial differences between the activation energies extracted from the SW surface (1.53 kcal mol^{-1}) and our findings[1] (1.32 kcal mol^{-1}). As noted in ref 2, not only is the exothermicity of the SW surface too small (by ca. 0.3 kcal mol^{-1}) but its barrier height is probably too low by ca. 0.4 kcal mol^{-1} (meaning the barrier of ref 1 is also too low).

Because a proper resolution of the differences between experiment and theoretical simulation depends on obtaining the best possible description of the $F + H_2 \rightarrow FH + H$ energy surface, we decided to attempt to determine, to an accuracy of 0.1 kcal mol^{-1}, this reaction's ground-state surface at certain geometries that are especially pertinent to experimental studies. In the present paper, we therefore extend the efforts of ref 1 in three primary directions:

1. We improved upon the treatment of electron correlation, with a goal of achieving an accuracy of 0.1 kcal mol^{-1}, by using

† Part of the special issue "Donald G. Truhlar Festschrift".

* To whom correspondence should be addressed. E-mail: simons@chem.utah.edu.

‡ Present address: Chemistry Department, Cornell University, Ithaca, NY.

§ North Carolina A&T State University, Department of Physics, Rm. 101, Marteena Hall, Greensboro, NC 27411.

10.1021/jp052318p CCC: $33.50
Published on Web 11/01/2005

explicitly correlated r_{12} methods that we have shown in earlier studies on N_2,[4] He_2,[5] Ne_2[6], and HF[7] are more than capable of this accuracy.

2. We included both spin−orbit and scalar relativistic corrections to the PES in a fashion similar to what Hartke and Werner added[8] to the SW surface to generate what we later denote as the HSW surface.

3. We computed such high-level explicitly correlated energies at ca. 228 geometries including near the F + H_2 → FH + H intrinsic reaction path (IRP) and in the neighborhoods of (a) the F···H_2 reactant van der Waals well, (b) the FH···H product van der Waals well, (c) the F + H_2 reactants and FH + H products, (d) as well as the transition state.

This paper is organized as follows. In section II, we describe succinctly the basis set, the electronic configuration active space (AS), and the correlation method we use and we describe how we selected the geometries where we performed explicitly correlated calculations. In section III, we give our results at the F + HH and FH + H asymptotes, the van der Waals minima, and the transition state. In the last section, we summarize our findings.

II. Methods

A. General. The explicitly correlated electronic structure calculations were performed using the AMICA suite of programs,[9] which is based on the Columbus program package.[10]

The molecular orbitals were optimized in a multiconfigurational self-consistent field (MCSCF) calculation. The orbital redundancies within the active orbital space were resolved by diagonalizing the generalized Fock matrix (denoted **Q**[11]). The MCSCF energies were converged to 10^{-10} E_h (Hartree units of energy), and the ACPF-2 and r_{12}-ACPF-2 energies were converged to 10^{-6} E_h. The scalar relativistic corrections were calculated using the Molpro[12] program, where the MCSCF and ACPF energies were converged to 10^{-10} E_h. All distances in this work are reported in atomic units (a_0).

The geometries of the F + H_2 system are expressed as in ref 1. In general, the geometry for each point on the F + H_2 PES can be expressed by three distances, r_{F-H}, $r_{H-H'}$ (r), and $r_{F-H'}$. In this paper, we use two additional ways to describe certain geometries. The transition state is described by r_{F-H}, $r_{H-H'}$ (r), and the angle θ complementary to the angle formed by the vectors $\mathbf{r}_{F-H}$ and $\mathbf{r}_{H-H'}$. In addition, Jacobi coordinates are used to describe geometries in the reactant channel. They consist of the distance $r_{H-H'}$ (r), the distance R between the center-of-mass of $r_{HH'}$ and the F atom, and the angle φ between the vectors associated with the distances r and R.

B. Basis Sets, Reference Space, and r_{12}-ACPF-2 Method. In ref 7, we calculated the Born−Oppenheimer potential for the ground state of the HF molecule using the r_{12}-ACPF-2 functional. At the same time, we were able to construct basis sets for HF that also could be used for the calculation of the F + H_2 PES. The new basis sets for F and H were constrained to both achieve high accuracy and to retain a degree of compactness that would allow us to also treat the larger system F + H_2. The basis set that was compiled for the HF molecule contained 304 uncontracted (spherical) Gaussian basis functions and had the following composition: F[18s13p8d6f4g3h2i] and H:[11s6p4d3f] (see ref 7). In the same paper, we examined convergence in the computed values of the dissociation energy D_e as the AS size and composition varied for the HF molecule. Next, this basis set and an AS containing 352 reference configuration state functions (CSFs) were used to calculate a nonrelativistic r_{12}-ACPF-2 potential for HF, which afterward was corrected for scalar relativistic effects (mass-velocity and Darwin correction) as well as for spin−orbit effects which proved to be nonnegligible due to the presence of a F atom. This combination of basis set, AS choice, and treatment of spin−orbit and relativistic effects resulted in very accurate calculated spectroscopic constants for the HF molecule.

To make the previous kind of explicitly correlated calculations feasible for use at many geometries on the F + H_2 PES, we needed to compress the basis set without losing significant accuracy. This became necessary because of the necessity to include multiple reference configurations in the wave function, the lower symmetry of this molecular system, and the computational cost of carrying out such calculations (e.g., calculating the r_{12}-ACPF-2 energy at a single geometry requires between 350 and 1400 h of CPU time even on our fastest computer, a 32-bit s1533 MHz dual-processor machine with 3 GB memory and 200 GB hard disk). We discovered that we could remove the *i*-symmetry basis functions on F and the *f*-symmetry functions on H without significantly affecting the computed D_e value (<0.1 kcal mol^{-1}) for HF. The basis set we then used to tackle the F + H_2 PES thus contains the following functions: [18s13p8d6f4g3h] for F and [11s6p4d] for H, which results in a total of 257 basis functions for the HF molecule and 306 basis functions for the F + H_2 system.

In ref 1, we also investigated the convergence of the active space with respect to the F + HH → FH + H reaction exothermicity and the barrier height by monitoring the energy of the reactants, the products, and the linear-constrained transition state. The issue of symmetry breaking, by which many of the active spaces we considered were eventually eliminated, posed a serious problem that we needed to overcome. We eventually identified several active spaces that were good candidates for the further study of the F + H_2 PES, and we selected one that would be most viable. In this earlier paper on the AS (ref 1), we used the notation (klmn/xwyz) to denote the number of *internal* (klmn) orbitals and the number of doubly occupied or *inactive* orbitals (xwyz) within the a_1, b_1, a_2, and b_2 symmetries of the C_{2v} point group. The orbitals that are internal but not constrained to be doubly occupied we term *active*. We also used the notation (pq/rs) to make a similar declaration of the a'- and a''-symmetry orbitals in the C_s point group. The AS space we selected for further use in the explicitly correlated treatment of F + H_2 is denoted as (7202/1000) in C_{2v} symmetry or (92/10) in C_s symmetry.

The 10 active orbitals involved in the AS have, at the F + H_2 asymptote, the character of F(2s,2p,3s,3p) and $H_2(\sigma_g,\sigma_u)$, while the F(1s) orbital is inactive. The reference CSFs that we use in our r_{12} calculations are created by forming all possible distributions of nine electrons among the F(2s,2p) and the H_2-(σ_g,σ_u) valence orbitals. As such, this space of CSFs is of complete active space (CAS) character. Additional reference CSFs are generated by carrying out single and double excitations of these valence orbitals into the higher lying F(3s,3p) orbitals (subject, of course, to spin- and spatial-symmetry constraints). From the (7202/1000|92/10) AS, a total of 1276 reference configurations were generated in C_{2v} symmetry and 2467 reference configurations were obtained in C_s symmetry using the approach outlined above.

In ref 1, where we investigated several ASs for the F + H_2 PES, we used this (92/10) AS and the ACPF-2 method to calculate several properties at especially interesting geometries on the F + H_2 PES. We found that the use of this (92/10) AS resulted in a better D_e for HF (141.0 kcal mol^{-1}) but an exothermicity for the F + H_2 → FH + H reaction (32.5 kcal

mol^{-1}) of similar quality to that obtained earlier from the Stark and Werner[3] data (140.3 and 31.8 kcal mol^{-1}, respectively), where the corresponding experimental data are 141.1 and 32.0 kcal mol^{-1}. These nagging discrepancies suggested to us that the subsequent r_{12}-ACPF-2 study detailed here would make even further improvements on our description of this reaction's PES and would thus help bring closer the experiment−simulation gap on this important test-case reaction.

All of the calculations for the F + H_2 surface that we report in this paper were performed in C_s symmetry, even at those geometries that possess C_{2v} symmetry. Without any further restrictions on the basis set or the number of reference configurations, the combination of the number of basis functions and reference configurations would generate a r_{12}- ACPF-2 wave function containing more than 709 million CSFs, a number far beyond present-day computing resources for calculating the entire PES. We therefore had to design a method to reduce the number of reference configurations without losing accuracy.

To this end, before carrying out r_{12}-ACPF-2 calculations at any geometry with our newly compiled basis set and AS choice, we first perform a MCSCF calculation using the 2467 CSFs in the reference AS, after which we carry out an ACPF-2 calculation based upon this 2467 CSF reference function using Dunning's aug-cc-pVQZ[13] basis. In these calculations, we do not correlate the F($1s^2$) core electrons to reduce the calculation time. We then reduce (below 2467) the number of reference CSFs for the final r_{12}-ACPF-2 calculation by selecting only those CSFs that have, in the above ACPF-2 wave function, an amplitude that surpasses a threshold of $\tau = 25 \times 10^{-6}$. Smaller thresholds made the subsequent explicitly correlated calculation unfeasible, while this value allowed us to achieve the final accuracy we desired (ca. 0.1 kcal mol^{-1}).

The use of such a threshold approach can lead to artificial "bumps" in the PES, in particular in areas where the curvature of the surface is rather flat. This might be also overcome by merging all of the reference CSFs whose amplitudes are greater than the threshold value over a range of geometries. In practice, the latter approach again generated too many CSFs to include in our subsequent r_{12}-ACPF-2 calculations. We therefore opted for a compromise in which we merged all the above-threshold CSFs within a given region of the PES (i.e., the van der Waals wells, the transition state, the reactants, and the products). We were thus able to optimize all of these geometrical structures without experiencing artificial "bumps".

After using the above strategy to select the reference CSFs at a given region of geometry, we perform a MCSCF calculation using the basis set we earlier described constructed for the r_{12} calculations (306 basis functions) and using the 2467 reference CSFs. We then use the optimized MCSCF orbitals (for the 2467 reference CSFs) to subsequently carry out the r_{12}-ACPF-2 calculation employing the previously selected reference CSFs using the MCSCF orbitals that were optimized for the 2467-CSF wave function. In the final r_{12}-ACPF-2 calculation, all of the electrons are correlated, including the F($1s^2$) pair.

Finally, the r_{12}-ACPF-2 calculation may give rise to instabilities[14] that can be controlled when we limit the number of independent r_{12} terms in the wave function by restricting the unitary invariance of the internal orbitals to certain disjoint subsets. In our calculations, we reduced the number of independent r_{12} variables by partitioning the space of the internal orbitals into three subsets: {F(1s)},{F(2s)} and {F(2p,3s,3p), $H_2(\sigma_g,\sigma_u)$}.

C. Selection of Geometries at which to Compute Explicitly Correlated Energies. As noted earlier, the r_{12}-ACPF-2 calculations are very computationally expensive. Therefore we needed to focus our computational efforts toward certain areas of the PES: the asymptotes where the energy variation tracks that of the diatomic H_2 and HF potentials, both van der Waals wells (reactant and product), as well as the bent transition state and the IRP connecting the transition state and both wells. We also carried out calculations along an IRP that connects the product well to the products because, in our exploration of the SW PES, we found small bumps in these regions that may very well be artificial. Finally, we also performed calculations over grids of points (detailed later) in the regions of the bent transition state (to obtain the local curvatures and to accurately locate the transition state) as well as in the van der Waals wells (again, to determine the curvatures and to accurately locate these minima).

The potential profile at the reactant asymptote was calculated by using a linear geometry and by keeping the F atom fixed at a distance of 100 a_0 from the nearest H atom and varying the $r_{HH'}$ distance. At such geometries, a total of 17 points in the range from 1.20 to 1.80 a_0 were calculated at the r_{12}-ACPF2 level using 49 reference configurations that were themselves obtained by merging all the reference configurations that surpass the threshold τ in the preceding ACPF-2 calculations at exactly the same geometries. In addition, to correctly describe the dissociation of the H_2 molecule and to obtain data at larger H−H separations representative of the FH···H van der Waals well, 12 more energies were calculated at 1.85, 1.90, 1.95, 2.00, 2.50, 3.00, 3.50, 4.00, 4.50, 5.00, 7.50, and 100.00 a_0, at which the same configuration threshold strategy (based on the same τ value) was employed. This produced a total of 29 energies relating to the variation along the H−H′ coordinate.

The potential profile in the FH + H′ product region was also calculated at a linear geometry by keeping the two H atoms 100 a_0 apart and varying the r_{FH} distance. Thirteen points in the range of 1.35 to 2.40 a_0 were calculated at the r_{12}-ACPF-2 level using 90 reference configurations obtained in the same way as for the reactant asymptote. To obtain data at larger F−H distances pertinent to the F···HH′ van der Waals well, we also calculated additional energies at 2.80, 3.00,3.50, 4.00, 4.50, 5.00, 7.50, and 100 a_0, again using the same threshold criterion (and the same τ) as discussed earlier**.** This produced a total of 21 energies.

The energies in the region (at 54 geometries) of the van der Waals well in the reactant channel were calculated by merging 52 reference CSFs identified by applying the threshold-selection process at 72 different geometries obtained in a preceding ACPF-2 calculation using 2467 reference CSFs. The r_{12}-ACPF-2 energies in the product well (at 40 geometries) were calculated using 94 reference CSFs chosen by merging the threshold-selected reference CSFs from ACPF-2 calculations at 60 different geometries (half of which deviated from the minimum-energy T-shaped structure) in the neighborhood of the well.

When continuing the IRP from the product well to the products, we found an unexpected bump in the SW surface. This same anomaly was observed in ref 2. To find out whether this was an artifact in the SW surface, we calculated a total of 15 energies within a grid defined by $r_{FH} = \{1.73, 1.735, 1.740\}$, $r_{HH'} = \{4.75, 5.0, 5.5, 6.0, 6.5\}$, and $\theta = 0°$. We again merged the reference CSFs that fulfilled our threshold criterion (to produce a total of 91 CSFs). Our results convinced us that the bump on the SW surface was indeed an artifact, which the authors of ref 2 also concluded.

To identify the important reference configurations near the transition state, we performed ACPF-2 calculations at 60 points within the 3D grid defined by $r_{FH} = \{2.88, 2.93, 2.98\}$, $r_{HH'} =$

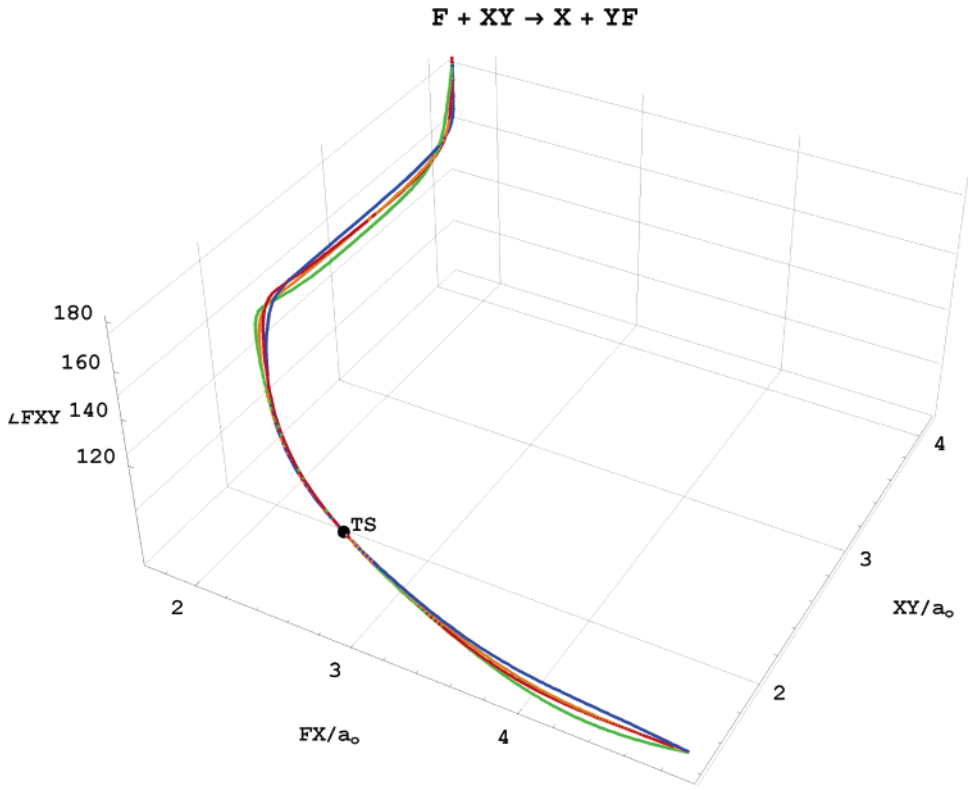

Figure 1. IRC for the F + H_2 reaction connecting the transition state to the van der Waals wells for various isotopes (X/Y = H/H, HD, DH, and DD) as functions of two distances and the bending angle.

{1.450, 1.455, 1.460, 1.465}, and θ = {58°, 61°, 64°, 67°, 70°}. We merged all the reference configurations that had a higher weight than the threshold τ in the ACPF-2 wave function, which resulted in a total of 177 configurations that were subsequently used to perform r_{12}-ACPF-2 calculations at 36 geometries within the same grid.

The geometries along the reaction path at which r_{12}-ACPF-2 calculations should be carried out were determined by first performing a "walk" on the SW PES along the IRC[15] starting from the transition state (TS) and connecting to both wells. Several algorithms (eigenmode, following[16−19] the Euler method, and the local quadratic approximation (LQA)[20] method) were implemented and tested on some benchmark surfaces such as the KMB[21] surface. We used each of these algorithms on the SW PES, and they resulted in virtually the same trajectories (as long as the step size was small and the same isotope was used). The IRC walk on the surface properly preserved the center-of-mass (COM), and the rotational motions were projected[10] out. The use of mass-weighted Cartesian coordinates allowed us to obtain the IRCs for the different H isotopes; as can be seen from Figure 1, the paths for all four trajectories deviate slightly, so we chose to use the F + HH IRC to carry out our r_{12}-ACPF-2 energy calculations.

In total, 34 geometries (each spaced by an energy of 1 kcal mol^{-1}) were sampled along the SW surface's IRC starting at the bent TS and ending in the FH + H product well. That is, each of the geometries has an energy that is 1 kcal mol^{-1} different from that of its neighbors. The reference CSFs for each geometry were those that had a higher weight than the threshold τ in the MR-ACPF-2 wave function containing 2467 CSFs at that geometry. We opted for this approach because the physical character of the reference CSFs changes considerably from the bent TS to the product well. Along the opposite direction of the IRC (i.e., starting from the bent TS and leading to the reactant well), we selected seven geometries spaced by 0.25 kcal mol^{-1}. We opted for a similar strategy as we chose for the product interval of the IRC—we only used those references that had a weight larger than τ in the ACPF-2 wave function.

We found that imposing the restriction of the unitary invariance among the internal orbitals employed in the construction of the r_{12} terms indeed improved the numerical stability of the r_{12}-ACPF-2 wave function significantly. Nevertheless, we found several points along the IRC were the r_{12}-ACPF-2 wave function "broke down" due to the presence of negative eigenvalues of the Hessian matrix constructed in the vector space of the trial vectors. The presence of one or more negative eigenvalues of the Hessian in cases where one is studying the ground state casts doubt on the validity of the energy. We noticed that this arose primarily around the transition barrier, especially when many reference CSFs were present (more than 180). We did not include any energies that were obtained when the program had not reached the 10^{-5} E_h convergence threshold or had displayed the irregular Hessian behavior discussed above.

III. Results and Discussion:

A. PES in the Asymptotic Regions. Our 228 r_{12}-ACPF-2 energies were also used to refine the parameters appearing in the two-body components of the functional form (ref 3) that expresses the SW PES as follows

$$V(R_{AB}, R_{BC}, R_{AC}) = \sum_i V_i^{(1)} + \sum_n V_n^{(2)}(R_n) + V_{ABC}^{(3)}(R_{AB}, R_{BC}, R_{AC})$$

The energies of the three individual atoms are expressed by $V_i^{(1)}$ (i = A(F), B(H), C(H′)), and the diatomic potentials are contained in the terms $V_n^{(2)}$ where n can be AB(FH), AC(FH′), or BC(HH′). The three-body contribution to the potential is expressed by $V^{(3)}$ (R_{AB}, $R_{AC,}$ R_{BC}) and, of course, is a function

TABLE 1: Parameters of Our Optimized Two-Body Potentials $V^{(2)}_{cgs}$ Followed by Those of the Original SW Surface

parameter	HF	H_2
D_e (hartrees)	0.22595580/0.22361367	0.17463024/0.17369212
a_1	2.310949901/2.34122333	2.17830163/2.19220027
a_2	1.307547917/1.36362029	1.30424354/1.36011506
a_3	0.665658077/0.74001884	0.70882425/0.69602488
a_4	0.0/0.0	0.17463024/0.17369212
R_e	1.73305288/1.73471165	1.39893899/1.40013039

of all three interatomic distances. Both two-body potentials have the same functional form as used in the SW surface

$$V_n^{(2)}(x) = -D_e(1 + a_1x + a_2x^2 + a_3x^3)e^{-a_1x} + a_4$$
$$x = R_n - R_n^e$$

but, of course, we obtained our own values for the parameters as described below. In each $V_n^{(2)}(x)$, a_1, a_2, a_3, and a_4 as well $R^{(e)}_n$ and D_e, the dissociation energy of the diatomic molecule, are parameters that have to be optimized. The a_4 parameters are chosen to make the potential zero at the minimum-energy structure (i.e., F + HH′) of the reactant asymptote, which is the same choice used by SW[3] in forming their potential. The values of R_e and of D_e for H_2 and FH were obtained from our r_{12}-ACPF-2 calculations; only the a_1, a_2, and a_3 parameters were obtained by fitting our H_2 and FH energies at other internuclear distances to the two-body functional form shown above. The a_4 parameter for FH is taken as 0.0 (to guarantee that the potential vanishes when H_2 is at its equilibrium bond length and F is 100 a_0 away), and a_4 for H_2 is taken as $D_e(H_2)$ to make the potential agree with our r_{12}-ACPF-2 computed exothermicity at the FH + H product geometry.

The other parameters of the $V_n^{(2)}$ were optimized by carrying out nonlinear optimizations using our 29 r_{12}-ACPF-2 energies at the reactant asymptote (F + HH′) to obtain the parameters in the HH′ diatomic potential and our 21 r_{12}-ACPF-2 energies at the product asymptote (FH + H′) to obtain the FH diatomic potential. The fit of our 29 r_{12}-ACPF-2 energies to the two-body potential of H_2 produced a fit with a root-mean-square (rms) accuracy of 0.09 kcal mol^{-1}. In fitting the data to obtain optimal parameters for the FH two-body potential, we found that a fit with an rms deviation of 0.04 kcal mol^{-1} was obtained if we employed only those 16 r_{12}-ACPF-2 energies ranging out to 3.0 a_0, including the r_{12}-ACPF-2 energies at the five points between 3.5 and 7.5 a_0 generated a fit with an rms deviation of 0.25 kcal mol^{-1}. Thus, consistent with our original goal of reporting r_{12}-ACPF-2 energies to 0.1 kcal mol^{-1}, we chose to include only data out to 3.0 a_0 and report modified SW two-body potentials that fit our data to the 0.1 kcal mol^{-1} accuracy, even if the range over which these fits is accurate might be limited to 3.0 a_0 or smaller.

The optimized parameters (assuming all energies are in hartrees and all distances are in a_0 units) that result from this process are given in Table 1 where we also give the original parameters of the SW two-body potentials.

Because the fit of the r_{12}-ACPF-2 data for FH produced rms errors exceeding 0.1 kcal mol^{-1} when the data points at distances exceeding 3.0 a_0 were included, we decided to extend the original three-parameter (a_1, a_2, a_3) SW two-body functional to include two additional terms thus producing a function of the following form

$$V_n^{(2)}(x) = -D_e(1 + a_1x + a_2x^2 + a_3x^3 + a_4x^4 + a_5x^5)e^{-a_1x} + a_6$$
$$x = R_n - R_n^e$$

We then fit all 29 of our H_2 and all 21 of our FH r_{12}-ACPF-2 energies to this functional and achieved rms errors of 0.09 and 0.13 kcal mol^{-1}, respectively, both of which allow these new potentials to represent our r_{12}-ACPF-2 data within the desired 0.1 kcal mol^{-1} specification. The optimal parameters for these new five-parameter two-body potentials are given in Table 2.

The actual r_{12}-ACPF-2 energies and HH′ distances (the F atom was held 100 a_0 from the nearest H atom) used in achieving this fit in the F + HH′ region are shown in Figure 2, as is the analytical fit itself. The point at $r_{HH'} = 100$ a_0 is not shown for convenience. We wish to stress that the range of HH′ distances where r_{12}-ACPF-2 energies were computed and where the potential fit remains accurate to 0.09 kcal mol^{-1} spans the equilibrium bond length of H_2, the HH′ distances in the FH···H′ and F···H_2 complexes, and the transition state.

We also wish to note that a comparison of our r_{12}-ACPF-2 energies and of the fits using the parameters reported above (either the fit of Table 1 or that of Table 2) to the highly accurate H_2 potential of Wolniewicz[22] shows that our potential function agrees with the results of ref 22 to within 0.09 kcal mol^{-1} out to 3.2 a_0 but deviates by 0.18 kcal mol^{-1} at 3.4 a_0 and by 0.21 kcal mol^{-1} at 5.0 a_0. Thus, our H_2 two-body potential function likely is accurate (i.e., fits our r_{12}-ACPF-2 data within this limit and our r_{12}-ACPF-2 data itself is accurate within this limit) to our stated 0.1 kcal mol^{-1} only for HH′ distances up to 3.2 a_0. This range is adequate for the reactants, the F···H_2 van der Waals well, and the transition state but is somewhat outside the HH′ distance (4.3 a_0) characterizing the FH···H′ van der Waals well.

The energies and FH distances (the H′ atom is held fixed 100 a_0 away from the H atom) used to obtain the parameters in the FH two-body potential given in Table 2 are shown in Figure 3 as is the analytical fit itself. Again, the point at $r_{FH} = 100$ a_0 is not shown for convenience. Note that the range of FH distances where r_{12}-ACPF-2 energies were computed and where our five-parameter fit is accurate to 0.1 kcal mol^{-1} spans the equilibrium bond length of FH, the FH distance in the F···HH′ and FH···H′ complexes, and the transition state.

From Figures 2 and 3, we see clearly that the two-body potentials for HF and H_2 are smooth and provide good representations of the r_{12}-ACPF-2 energies, which have been shifted to render the potential energy zero at the F + H_2 asymptote when HH′ is at its minimum. The rms errors pertaining to the five-parameter two-body potentials for HH′ and FH detailed above are 0.1 kcal mol^{-1} within the range of internuclear distances characterizing both van der Waals wells and the transition state. Moreover, the HH′ potential also agrees within 0.1 kcal mol^{-1} with the data of ref 22 over the most important range of HH′ distances. These findings suggest that our new five-parameter two-body potentials will be appropriate to use in a next-generation 3D surface for the F + H_2 → FH + H surface.

B. Spin−Orbit and Scalar Relativistic Corrections. In our earlier study of the ground state of the HF molecule,[7] we corrected the energies for the spin−orbit and scalar relativistic contributions, the latter being composed of the mass-velocity and Darwin corrections. The sum of the scalar relativistic and spin−orbit corrections we term the total relativistic contribution.

TABLE 2: Parameters of Our Optimized Five-Parameter Two-Body Potentials $V^{(2)}_{cgs}$ Followed by Those of the Original SW Surface

parameter	HF	H_2
D_e (hartrees)	0.22595580/0.22361367	0.17463024/0.17369212
a_1	2.67367460/2.34122333	2.32576382/2.19220027
a_2	2.18700104/1.36362029	1.63942330/1.36011506
a_3	1.33651504/0.74001884	0.88964381/0.69602488
a_4	0.49050336/0.0	0.15574627/0.0
a_5	−0.06175378/0.0	0.00001245/0.0
a_6	0.0/0.0	0.17463024/0.17369212
R_e	1.73103141/1.73471165	1.39978507/1.40013039

In the present study, we will consider the same two important relativistic effects.

After verifying their quality at a number of geometries by carrying out our own calculations, we took the spin−orbit corrections directly from the work from Hartke and Werner,[8] who calculated this correction in those regions where it is most significant (i.e., in the reactant channel where the F atom's spin−orbit energy is large—the $^2P_{3/2}-^2P_{1/2}$ splitting[23] is 404 cm^{-1}). We calculated the scalar relativistic correction at 1380 geometries defined by a 3D grid formed by taking 23 points along the r_{FH} axis (ranging from 1.35 to 100.00 a_0), 12 points along the $r_{HH'}$ axis (ranging from 1.20 to 100.00 a_0), and 5 angles $\theta = \{0°, 30°, 60°, 90°, 120°\}$. To keep these calculations feasible, we used the aug-cc-pCVQZ[24] basis set for F and the aug-cc-pVQZ[13] basis set for H instead of the more expensive aug-cc-pCV5Z[24] and aug-cc-pV5Z[13] basis sets that we used in our earlier study of HF.[7] We justify this choice of basis by noting that the D_e values of HF computed using the two respective bases and adding the resultant scalar relativistic corrections to the r_{12}-ACPF-2 energies are 0.205 and 0.197 kcal mol^{-1} below the values obtained using the r_{12}-ACPF-2 data alone, so results from the two bases are indeed very similar.

In our investigation of the AS for the F + H_2 PES,[1] we found many ASs suffer from symmetry breaking. Therefore, we did not use the kind of valence-CAS AS that we used earlier for the HF molecule.[7] Instead, we chose the smallest AS that was found in ref 1 to be able to correctly describe the entire F + H_2 PES and to be free from symmetry breaking. This was a reference space composed of the following active orbitals: F(2s,2p,3p) and $H_2(\sigma_g,\sigma_u)$, with the F(1s) orbital being inactive. To limit the number of reference configurations, we performed all possible excitations within the subspace spanned by the F(2s,-2p) and $H_2(\sigma_g,\sigma_u)$ orbitals but only included single and double excitations out of this subspace into the F(3p) orbitals. The resulting AS is denoted (6202/1000|82/10) and contains 1464 reference CSFs. In the subsequent ACPF-2 calculations, we correlate all electrons and the mass-velocity and Darwin corrections are then calculated as expectation values over the ACPF wave function. We then formed the total relativistic correction by adding the spin−orbit correction of Hartke and Werner[8] to our calculated scalar relativistic correction.

The spin−orbit energies calculated by Hartke and Werner are largely situated in the reactant channel, which covers only that part of the PES where the spin−orbit correction is significant. In contrast, the scalar relativistic contribution is most significant in the product-channel region of the PES. We therefore determined the spin−orbit correction at all of the 1380 geometries noted above using Hartke and Werner's 3D-spline program. These spin−orbit energies were then added to our scalar relativistic values at the same geometries. The total relativistic correction for each of these 1380 geometries was then used as input to Hartke and Werner's 3D-spline program to generate a new spline interpolation that allowed us to calculate the total relativistic correction for any geometry on the PES. The relativity-corrected energies for any geometry are then calculated by adding the relativistic correction to the nonrelativistic energies.

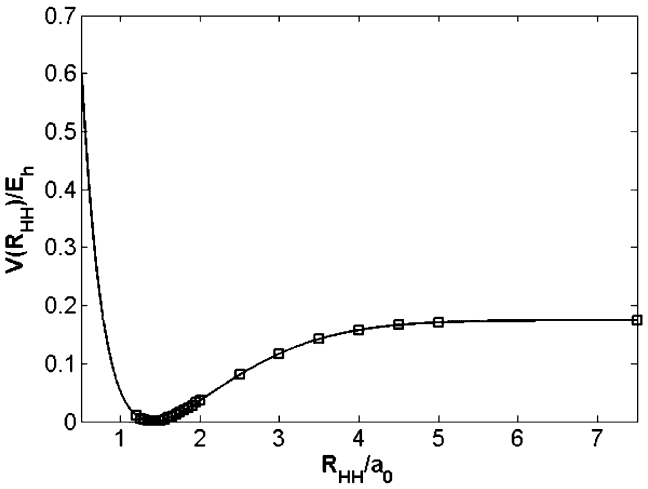

Figure 2. Diatomic potential for the H_2 molecule. The squares represent the r_{12}-MR-ACPF-2 energies (shifted by 100.90646839 hartrees); the curve is the diatomic H_2 potential reproduced using our parameters from Table 2 in the two-body functional form given in the text.

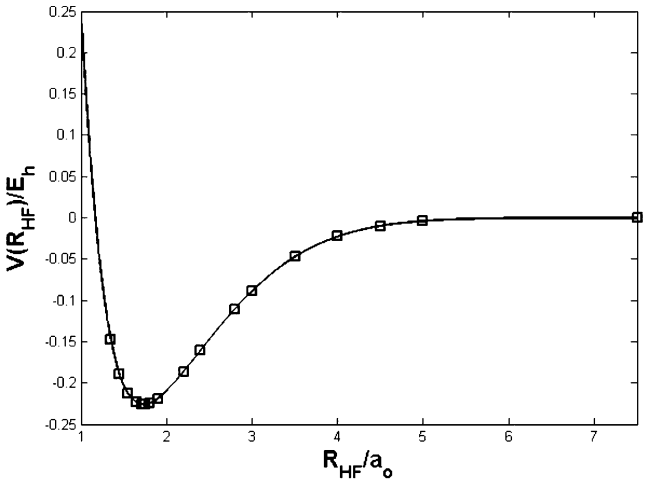

Figure 3. Two-body for the FH + H′ asymptote. The squares represent the r_{12}-MR-ACPF-2 energies (shifted by 100.90646839 hartrees); the curve is the HF two-body potential with our parameters from Table 2.

C. Diatomic Potential Parameters of H_2 and HF, the Reaction Exothermicity, and the Barrier Heights. In Figures 2 and 3, the nonrelativistic diatomic potentials for H_2 and HF are depicted for a wide range of internuclear distances. The r_{12}-ACPF-2 energy data underlying these nonrelativistic potentials, when corrected for relativistic effects as outlined above, allowed us to extract various spectroscopic parameters at this high level. The equilibrium bond lengths R_e and the harmonic frequencies ω_e were calculated by fitting the relativity-corrected r_{12}-ACPF-2 energies to quartic polynomials in R^{-1}

$$V(R) = \sum_{i=0}^{4} c_i R^{-1}$$

The distance R_e was obtained by finding the minimum in this quartic polynomial. The harmonic frequency ω_e was calculated from the second derivative of this quartic polynomial at the minimum, using atomic masses in order to simulate non-Born−

TABLE 3: Spectroscopic Constants of H_2 and HF, as well as the Reaction Exothermicity ($-\Delta E$) at the r_{12}-ACPF-2 (with and without relativistic correction) Levels and Comparison to Other Results

	H_2			HF			exothermicity
	r_e/a_0	ω_e/cm^{-1}	D_e/kcal mol^{-1}	r_e/a_0	ω_e/cm^{-1}	D_e/kcal mol^{-1}	$-\Delta E$/kcal mol^{-1}
r_{12}-ACPF-2 + REL[a]	1.401	4406	109.6	1.733	4133	141.2	32.01[b]
r_{12}-ACPF-2	1.401	4407	109.6	1.732	4136	141.8	32.60[b]
ACPF-2[i]	1.402	4456	109.0	1.735	4138	141.0	32.45
ASW[26]	1.400	4413[c]	109.7[d]				31.34
SW[3]	1.400	4404	109.0	1.734	4131	140.3	31.77
experiment	1.401[e]	4401[e]	109.5[e]	1.732[f]	4138[g]	141.1[h]	32.00 ± 0.02[i]

[a] Spin−orbit and scalar relativity corrected. [b] Calculated as $D_e(HF) - D_e(H_2) - {}^1/_2\,[\omega_e(HF) - \omega_e(H_2)]$. [c] Fit to $E(v) = \omega_e(v + {}^1/_2) - \omega_e x_e(v + {}^1/_2)^2 + \omega_e y_e(v + {}^1/_2)^3$ (Table 3 in ref 26). [d] Calculated as $D_0 + E(v = 0)$ (Table 3 in ref 26). [e] Huber and Herzberg.[27] [f] Coxon and Ogilvie (1989).[28] [g] Le Roy.[29] [h] Zemke et al. (1991)[30] [i] Calculated as $|D_0(HF^{30}) - D_0(H_2^{31})|$.

TABLE 4: Geometries and Energies (relative to F + H_2) for the Bent Barrier Obtained Using r_{12}-ACPF-2 (with and without relativistic correction) and Comparison to Existing Results

	bent barrier geometry and energy			
method	$r_{HH'}/a_0$	r_{FH}/a_0	θ/deg	$E^{\ddagger}$[a]
r_{12}-ACPF-2 +REL[b]	1.454	2.898	62.7	1.80
r_{12}-ACPF-2	1.454	2.900	62.6	1.42
ACPF-2	1.458	2.923	62.1	1.32
ASW/H_{so}[c]	1.457	2.916	64.1	1.92
ASW[26]	1.457	2.916	64.5	1.55
HSW[32]	1.458	2.914	62.0	1.91
SW[3]	1.457	2.922	61.0	1.53

[a] In kcal mol^{-1}. [b] Spin−orbit and scalar relativity corrected. [c] ASW results of ref 26 including spin−orbit corrections.

Oppenheimer effects.[25] To form the above quartic fits, we used energies at the following distances for the HF molecule: $r_{HF} = \{1.71, 1.72, 1.73, 1.74, 1.75\}$, all of which are very close to the equilibrium bond length. For the H_2 molecule, we used energies computed at $r_{HH'} = \{1.38, 1.39, 1.40, 1.41, 1.42\}$, again using data very near the equilibrium bond length. In each case, we kept the third atom at least 100 a_0 away from the two other atoms. In Table 3, our results are compared with some results from the literature.

A few observations about these findings are in order. First, we note that the D_e values for H_2 and HF and the reaction exothermicity, when computed at the relativity-corrected r_{12}-ACPF-2 level, are all within 0.1 kcal mol^{-1} of the experimental values, although results excluding relativity or excluding explicit correlation are not. Second, the spin−orbit and other relativistic corrections to the reaction exothermicity are ca. 0.6 kcal mol^{-1}, so they are essential to include if an accuracy of 0.1 kcal mol^{-1} is desired.

In Table 4, the r_{12}-ACPF-2 transition-state geometries and energies (with and without relativistic corrections) are presented, as are the results from several other PESs and calculations. To find the transition state, the r_{12}-ACPF-2 energies and the relativity-corrected energies were calculated on a 3D grid formed by $r_{HH'} = \{1.45, 1.455, 1.460\}$, $r_{FH} = \{2.88, 2.93, 2.98\}$, and $\theta = \{61, 64, 67\}$ and fit to a second-order polynomial in the three interatomic distances $r_{HH'}$, r_{FH}, and $r_{FH'}$. We optimized the polynomial with respect to the three independent variables and obtained a saddle point of first order.

Although the r_{FH} and $r_{HH'}$ values at the transition states do not depend much on the level of correlation or upon the inclusion of relativistic effects, we note that the activation barriers and the geometry angle do. In particular, it appears that including spin−orbit and other relativistic effects alters the barrier heights by ca. 0.4 kcal mol^{-1} (this was also noted in ref 2) whereas the inclusion of explicit correlation makes changes in the 0.1−0.2 kcal mol^{-1} range. Because these barrier heights play crucial roles in determining the reaction rates, it is essential that they be accurately described. Of course, the geometry of the transition state can play a role in determining the vibration−rotation state populations of the product HF molecules, so knowing it to high accuracy (as Table 4 suggests we do) will be helpful.

TABLE 5: Geometries and Well Depths (δE relative to the respective asymptotes) for Both van der Waals Wells and Comparison with Results of Previous Calculations

	F···H2				FH···H			
	r/a_0	R/a_0	φ/deg	δE[a]	$r_{HH'}/a_0$	r_{FH}/a_0	θ/deg	δE[a]
r_{12}-ACPF-2 + REL[b]	1.40	5.42	90.00	0.13	4.29	1.73	0.0	0.25
r_{12}-ACPF-2	1.402	4.87	90.00	0.30	4.29	1.73	0.00	0.25
ACPF-2	1.404	4.73	90.00	0.41	4.23	1.74	0.00	0.31
ASW/H_{so}	1.40	5.31	90.00	0.17				
ASW[26]	1.40	4.80	90.00	0.35				
HSW[32]	1.40	5.39	90.00	0.17				
SW[3]	1.40	4.77	90.00	0.36	4.19	1.74	0.00	0.25

[a] kcal mol^{-1}. [b] Spin−orbit and scalar relativity corrected.

The geometry and energy of the van der Waals well in the reactant channel computed at the r_{12}-ACPF-2 level were obtained by minimizing a second-order polynomial in r (the distance between the two hydrogen atoms) and R (the distance from the F atom to the center of mass of the H_2 bond). For the nonrelativistic energies, the grid at which energies were computed was formed by $r = \{1.40, 1.405, 1.41\}$ and $R = \{4.85, 4.90, 4.95\}$; for the relativity-corrected energies, the R grid was extended to $R = 5.50$ a_0. Because the spatial variation of the r_{12}-ACPF-2 energies in the region of this well was comparable in magnitude to the variation of the spin−orbit contribution, we observed substantial changes in the location and depth of this well when relativistic effects were included. In particular, the minimum shifted to larger R values and the well became shallower upon inclusion of relativistic contributions.

The location and depth of the van der Waals well in the product channel were determined by the optimization of a second-order polynomial in $r_{HH'}$ and r_{FH} using energies computed on a grid formed by $r_{HH'} = \{4.25, 4.30, 4.35\}$ and $r_{FH} = \{1.73, 1.735, 1.74\}$. In Table 5, our results for both van der Waals wells are presented and compared to the outcomes of other calculations.

We note that the geometry and depth of the product-channel van der Waals well vary little as the level of correlation is changed as well as when spin−orbit and other relativistic effects are included. In contrast, these properties of the reactant-channel well are strongly affected by electron correlation and relativity. Perhaps this is understandable given that in this well we have a nearly intact F atom (with substantial spin−orbit energy). We

also note that the depth of the FH···H well found in the present study is in reasonable agreement with the findings (0.27 to 0.32 kcal mol^{-1}) recently reported in ref 2.

VI. Summary

In this paper, we used an active space of electronic configuration state functions identified in our earlier work combined with a large and flexible orbital basis also tested earlier to compute ground-state Born−Oppenheimer energies for the F + HH′ → FH + H′ reaction. These calculations were performed using an explicitly correlated method at a large number of geometries characterizing the F + H_2 reactants, the F···H_2 and FH···H′ van der Waals complexes, the transition state, and the FH + H′ products, as well as at points along the intrinsic reaction coordinate connecting all of these stationary points. In addition, spin−orbit and scalar relativistic corrections to these energies were obtained. A total of 228 such energies were computed at various geometries.

Our results allowed us to construct highly accurate two-body contributions to the potential energy surface characterizing the above reaction. These potentials produce bond lengths, vibrational frequencies, and dissociation energies for H_2 and HF that agree with experimental findings to very high levels (e.g., within 0.1 kcal mol^{-1} for D_e). We were also able to provide a detailed characterization (e.g., geometries and well depths) of the two van der Waals complexes as well as the reaction's transition state (e.g., geometry and barrier height (1.8 kcal mol^{-1})). Finally, our computed exothermicity, when corrected for spin−orbit and other relativity effects (32.0 kcal mol^{-1}), is also within 0.1 kcal mol^{-1} of the experimental result. All of these findings suggest to us that our calculated energies are accurate to ca. 0.1 kcal mol^{-1}.

Acknowledgment. Support of the National Science Foundation through Grant CHE 0240387 is appreciated as is significant computer time provided by the Center for High Performance Computing at the University of Utah.

References and Notes

(1) Cardoen, W.; Gdanitz, R. J.; Simons, J. The F + H_2 → FH + H potential energy surface: proper construction of the electronic configuration space. *Int. J. Quantum Chem.*, in press.

(2) Hayes, M.; Gustafsson, M.; Mebel, A. M.; Skodje, R. T. *Chem. Phys.* **2005**, *308*, 259−266.

(3) Stark, K.; Werner, H.-J. *J. Chem. Phys.* **1996**, *104*, 6515−6530.

(4) Gdanitz, R. J. *Chem. Phys. Lett.* **1998**, *283*, 253−261.

(5) Gdanitz, R. J. *Mol. Phys.* **1999**, *96*, 1423−1434.

(6) Gdanitz, R. J. *Chem. Phys. Lett.* **2001**, *348*, 67−74.

(7) Cardoen, W.; Gdanitz, R. J. Accurately solving the electronic Schrödinger equation of atoms and molecules using explicitly correlated (*r*12)-MR-CI. VII. The hydrogen fluoride molecule. *J. Chem. Phys.*, in press.

(8) Hartke, B.; Werner, H.-J. *Chem. Phys. Lett.* **1997**, *280*, 430−438.

(9) Gdanitz, R. J. Amica ("Atoms & Molecules In Chemical Accuracy") suite of r_{12}-MR-CI programs, unpublished, 1997. Amica is distributed freely through the Internet site http://gdanitz.hec.utah.edu/amica.

(10) Lischka, H.; Shepard, R.; Shavitt, I.; Brown, F. B.; Pitzer, R. M.; Ahlrichs, R.; Böhm, H.-J.; Chang, A. H. H.; Comeau, D. C.; Gdanitz, R.; Dachsel, H.; Ehrhard, C.; Ernzerhof, M.; HÄochtl, P.; Irle, S.; Kedziora, G.; Kovar, T.; Müller, Th.; Parasuk, V.; Pepper, M.; Scharf, P.; Schiffer, H.; Schindler, M.; Schüler, M.; Szalay, P.; Dallos, M.; Zhao, J.-G. *Columbus*, an ab initio electronic structure program, release 5.4; 1998.

(11) Shepard, R.; Lischka, H.; Szalay, P. G.; Kovar, T.; Ernzerhof, M. *J. Chem. Phys.* **1992**, *96*, 2085−2098.

(12) *Molpro* is a package of ab initio programs written by Werner, H.-J.; Knowles, P. J. with contributions from Almlöf, J.; Amos, R. D.; Berning, A.; Deegan, M. J. O.; Eckert, F.; Elbert, S. T.; Hampel, C.; Lindh, R.; Meyer, W.; Nicklass, A.; Peterson, K.; Pitzer, R.; Stone, A. J.; Taylor, P. R.; Mura, M. E.; Pulay, P.; Schuetz, M.; Stoll, H.; Thorsteinsson, T.; Cooper, D. L.

(13) Dunning, T. H. *J. Chem. Phys.* **1989**, *90*, 1007−1023.

(14) Cardoen, W.; Gdanitz, R. J. *Comput. Methods Sci. Technol.* **2003**, *9* (1−2), 31−43.

(15) Fukui, K. *Acc. Chem. Res.* **1981**, *14*, 363−368.

(16) Cerjan, C. J.; Miller, W. H. *J. Chem. Phys.* **1981**, *75*, 2800−2806.

(17) Simons, J.; Jørgensen, P.; Taylor, H.; Ozment, J. *J. Phys. Chem.* **1983**, *87*, 2745−2753.

(18) Banerjee, A.; Adams, N.; Simons, J.; Shepard, R. *J. Phys. Chem.* **1985**, *89*, 52−57.

(19) Nichols, J.; Taylor, H.; Schmidt, P.; Simons, J. *J. Chem. Phys.* **1990**, *92*, 340−346.

(20) Page, M.; McIver, J. W., Jr. *J. Chem. Phys.* **1988**, *88*, 922−935.

(21) Müller, K.; Brown, L. D. *Theor. Chim. Acta* **1979**, *53*, 75−93.

(22) Wolniewicz, L. *J. Chem. Phys.* **1993**, *99*, 1851−1868.

(23) National Institute of Standards and Technology: Atomic Spectra Database.

(24) Dunning, T. H., Jr. *J. Chem. Phys.* **1995**, *103*, 4572−4585.

(25) Müller, H.; Franke, R.; Vogtner, S.; Jaquet, R.; Kutzelnigg, W. *Theor. Chem. Acc.* **1998**, *100*, 85−102.

(26) Alexander, M. H.; Manolopoulos, D. E.; Werner, H.-J. *J. Chem. Phys.* **2000**, *113*, 11084−11100.

(27) Huber, K. P.; Herzberg, G. *Constants of diatomic molecules;* Van Nostrand Reinhold: New York, 1979.

(28) Coxon, J. A.; Ogilvie, J. F. *Can. J. Spectrosc.* **1989**, *34*, 137.

(29) Le Roy, R. J. *J. Mol. Spectrosc.* **1999**, *194*, 189−196.

(30) Zemke, W. T.; Stwalley, W. C.; Coxon, J. A.; Hajigeorgiou, P. G. *Chem. Phys. Lett.* **1990**, *177*, 412−418.

(31) Balakrishnan, A.; Smith, V.; Stoicheff, B. P. *Phys. Rev. Lett.* **1992**, *68*, 2149−2152.

(32) Castillo, J. F.; Hartke, B.; Werner, H.-J.; Aoiz, F. J.; Banares, L.; Martinez-Haya, B. *J. Chem. Phys.* **1998**, *109*, 7224−7237.